

Normal Anatomy and Imaging of the Hip: Emphasis on Impingement Assessment

Mary Kristen Jesse, MD¹ Brian Petersen, MD² Colin Strickland, MD¹ Omer Mei-Dan, MD³

¹Division of Musculoskeletal Radiology, Department of Radiology, University of Colorado, Aurora, Colorado

²Division of Musculoskeletal Radiology, Department of Radiology and Orthopaedics, University of Colorado, Aurora, Colorado

³Division of Sports Medicine and Hip Preservation, Department of Orthopaedics, University of Colorado, Aurora, Colorado

Address for correspondence Brian Petersen, MD, Division of Musculoskeletal Radiology, Department of Radiology and Orthopaedics, University of Colorado, Stop L954, 12401 East 17th Ave, Room 5-006, Aurora, CO 80045
(e-mail: brian.petersen@ucdenver.edu).

Semin Musculoskelet Radiol 2013;17:229–247.

Abstract

Keywords

- ▶ hip anatomy
- ▶ hip imaging
- ▶ femoroacetabular impingement measurements
- ▶ hip dysplasia measurements

A comprehensive knowledge of normal hip anatomy and imaging techniques is essential in the evaluation and assessment of the patient with hip pain. This article reviews the osseous, soft tissue, and vascular components of the hip and the normal anatomical variants encountered in routine hip imaging. Basic and advanced hip imaging is discussed with particular emphasis on radiographic and computed tomography measurements and their utility in evaluating patients with developmental hip dysplasia and femoroacetabular impingement syndrome.

The hip serves as the essential focus of ambulatory movements and primary fulcrum for pelvic inclination and balance. A unique ball-and-socket morphology formed by the rounded head of the femur and cup-like pelvic acetabulum helps maintain proper pelvic tilt and allows for the dynamic range of rotatory motion including flexion, extension, abduction, and adduction. Given the magnitude of axial and rotatory load applied with bipedal physical activity, the concert of supporting ligaments, tendons, and muscles is crucial to maintaining hip joint strength and stability during ambulation. This article reviews the normal osseous and soft tissue anatomy of the hip, explores imaging options when evaluating the hip in routine clinical practice, and catalogs the ever-expanding list of routine measurements with which the musculoskeletal radiologist should be familiar when evaluating the active patient with hip pain.

Hip Anatomy and Normal Variants

Bones and Cartilage

The acetabulum is made up of a junction of three bones: the pubis medially, the ischium inferiorly, and the ilium superiorly. The Y-shaped secondary ossification center formed by the junction of these bones, the triradiate cartilage, is fused

uniformly at ages 12 to 16.^{1,2} The acetabulum forms the socket of the ball-and-socket joint, and aside from the acetabular notch inferiorly, it covers the entirety of the femoral head. The transverse acetabular ligament spans the osseous gap at the inferior acetabular notch forming a complete bony and ligamentous ring around the spherical femoral head. The acetabular cup is normally oriented inferiorly, laterally and anteriorly, directly opposing the superior medial orientation of the femoral head creating the inherently stable spheroidal joint configuration.

Acetabular and femoral articulating surfaces are lined by a durable lubricated layer of hyaline cartilage. The acetabular cartilage is interrupted centrally at the acetabular fossa that is filled with fibrofatty material called the pulvinar. The continuous femoral head cartilage is interrupted focally at the fovea capitis of the femoral head. Acetabular cartilage, also called the lunate cartilage due to the crescent or horseshoe shape, is more robust than femoral head cartilage with the greatest thickness along the superior lateral articular surface. The opposed femoral head cartilage demonstrates an opposite distribution with the area of greatest thickness along the superior medial articulating surface.³

A normal variation of the acetabular articular surface deserves special mention. Various names have been applied

Issue Theme Update in Hip Imaging; Guest Editor, Donna G. Blankenbaker, MD.

Copyright © 2013 by Thieme Medical Publishers, Inc., 333 Seventh Avenue, New York, NY 10001, USA.
Tel: +1(212) 584-4662.

DOI <http://dx.doi.org/10.1055/s-0033-1348090>.
ISSN 1089-7860.



Figure 1 Coronal T2 fat-saturated image of the hip in a young patient demonstrates a large type 1 supraacetabular fossa seen as a large focal defect in the acetabular cartilage and subchondral bone (arrow).

to an area of indentation or thinning of the central superior portion of the acetabular hyaline cartilage and subchondral bone; stellate lesion, stellate crease, supraacetabular fossa, and pseudodeflect of the acetabulum have all been used interchangeably in the literature. We define the stellate crease as a common arthroscopic finding of shallow cartilage deficiency just above the acetabular fossa, commonly not visible by imaging, and reserve the term *supra-acetabular fossa* (SAF) to describe a focal area of subchondral bony deficiency at the 12 o'clock position of the acetabulum. Two types of SAF have been described.⁴ Type 1 lacks cartilage infilling, allowing gadolinium or joint fluid to fill the defect (►Fig. 1) and is

typically seen in the young. These defects will eventually fill in with cartilage leading to the appearance of a type 2 SAF, which demonstrates normal cartilage but persistent subchondral bony indentation.

Bony protuberances about the femur and acetabulum serve as attachment sites for the stabilizing hip musculature. The greater trochanter of the femur consists of four facets: anterior, lateral, posterior, and superoposterior, serving as attachments for the abductor muscles (►Fig. 2). The gluteus minimus muscle attaches to the anterior facet, and the gluteus medius muscle attaches to the superoposterior and lateral facets. The lesser trochanter projects medially from the posterior inferior femoral neck shaft junction, and it serves as the insertion site for the primary hip flexor, the iliopsoas muscle.

Of the few osseous anatomical variants encountered in the hip, acetabular ossicles are the most common and most controversial. There are several developmental ossification centers of the acetabulum. These have been described anteriorly at the junction of the iliac and pubic bones (*os acetabuli anterius*), posteriorly at the junction of the iliac and ischial bones (*os acetabuli posterius*), and at the site of the triradiate cartilage (*os acetabuli central*).⁵ The literature suggests these normal variants occur in 2 to 3% of the population, and are often asymptomatic.⁶

Os acetabuli is commonly used to describe any ossification along the acetabular rim. This is controversial because many believe that acetabular rim ossification is the result of stress fracture related to hip impingement,^{7,8} hip dysplasia⁹ (►Fig. 3a, b), or chondro-ossification of the labrum related to impingement and/or subsequent to degenerative joint disease¹⁰ (►Fig. 3c). In our experience, acetabular, periacetabular, or labral calcification/ossification is quite common in the population of hip pain patients, and caution should be taken in discounting this finding as a normal variant. *Os acetabuli* has been suggested as a predisposing factor to pincer-type femoroacetabular impingement (FAI), but the

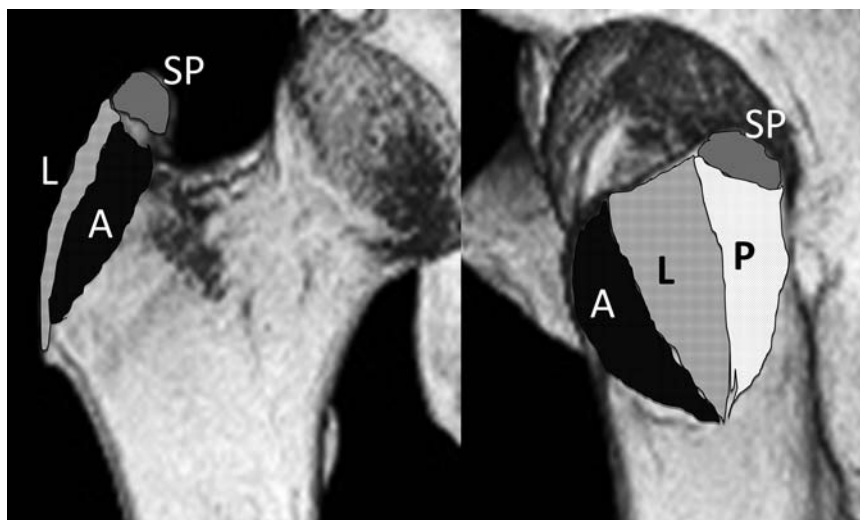


Figure 2 Anteroposterior and coronal three-dimensional reformatted images of the hip illustrating the four greater trochanteric facets: A, anterior; L, lateral; P, posterior; SP, superoposterior.

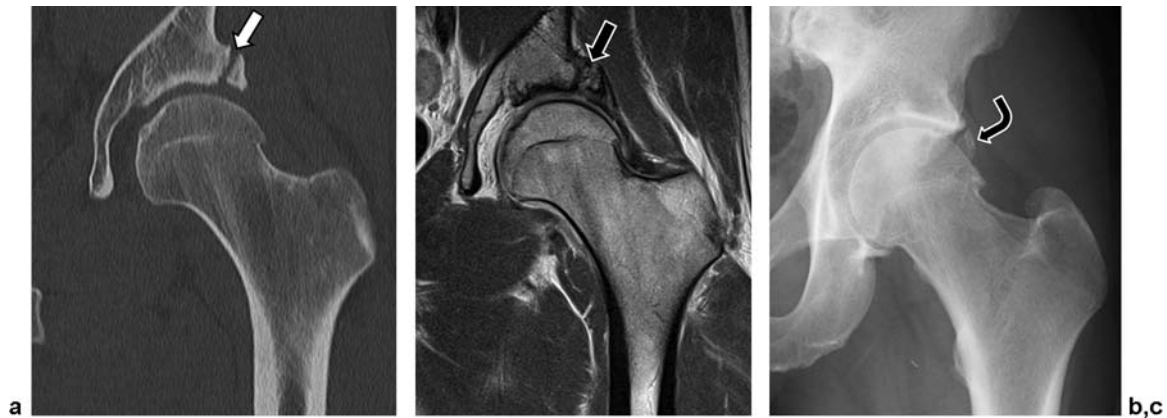


Figure 3 Examples of os acetabuli mimickers. (a) Coronal bone algorithm computed tomography and (b) coronal T1-weighted MR images of the left hip in a 33-year-old man with hip dysplasia and ongoing hip pain demonstrates sagittally oriented stress fracture of the superior acetabular rim related to developmental dysplasia of the hip (arrows). (c) Anteroposterior radiograph of the left hip in a 66-year-old man demonstrates ossification of the labrum in the setting of hip osteoarthritis (black curved arrow) that was symmetrical to his contralateral side (not pictured).

reverse may be more accurate—femoroacetabular impingement may result in labral or perilabral ossification producing the “os acetabuli” appearance.

Labrum

The labrum is a fibrocartilaginous structure lining the outer rim of the acetabular cup that blends with the transverse ligament along the inferior margin. Functionally, the labrum deepens the acetabular cup, improves hip joint stability, and distributes the synovial fluid to provide frictionless movement. Unlike the shoulder, the labrum of the hip does not appear to confer additional stability related to suction phenomenon.¹¹ The normal labrum consists of triangular shaped well-margined fibers that are thickest along the posterior aspect of the hip joint and thinnest anteroinferiorly.^{12–14} The

labrum is innervated by the obturator nerve and a branch of the nerve to the quadratus femoris. Nerve fibers are most densely compact in the anterior superior quadrant accounting for the painful nature of these lesions.¹⁵ The labrum blends with the hyaline cartilage of the acetabular cup along the deep margin, and it variably blends with the joint capsule and transverse ligament along the superficial margin. The variation in labral attachment to the transverse ligament gives rise to the labroligamentous sulcus, which should not be confused with a labral tear (→Fig. 4).^{16,17} The variable attachment of the superior joint capsule, commonly several millimeters above the labrum, creates the well-described prominent superior perilabral recess (→Fig. 5). Although similar perilabral recesses are found along the entire circumference of the labrum, they are typically smaller in the anterior and posterior quadrants given a more intimate capsulolabral attachment at the labral base.

Understanding normal variability in the labral morphology and signal is crucial in the accurate diagnosis of labral tears. Labral tears most commonly occur in the anterior superior and lateral quadrants of the labrum. Unfortunately, these areas have been shown in studies of asymptomatic patients to be the most affected with age-related morphological and signal changes. There is an age-related morphological trend from the normal triangular shaped labrum to a more rounded or hypoplastic anterior superior labrum.¹⁸ Similarly, increased intralabral signal in these areas was noted with aging,^{14,18,19} and this has been attributed to myxoid degeneration.¹⁹ These studies clearly complicate the radiologist's ability to discern symptomatic labral abnormality from asymptomatic age-related changes.

The cause and significance of the absent anterosuperior labrum (labral hypoplasia) noted to occur in 10 to 14% of asymptomatic patients^{14,18} is debated. Supporters suggest that labral hypoplasia may represent the hip equivalent of the Buford complex of the shoulder or reflect sequela of chronic repetitive tearing, as suggested by the age-related prevalence in prior studies.^{18,19} The actual existence of the labral hypoplasia entity has been called into question,^{20,21} and the

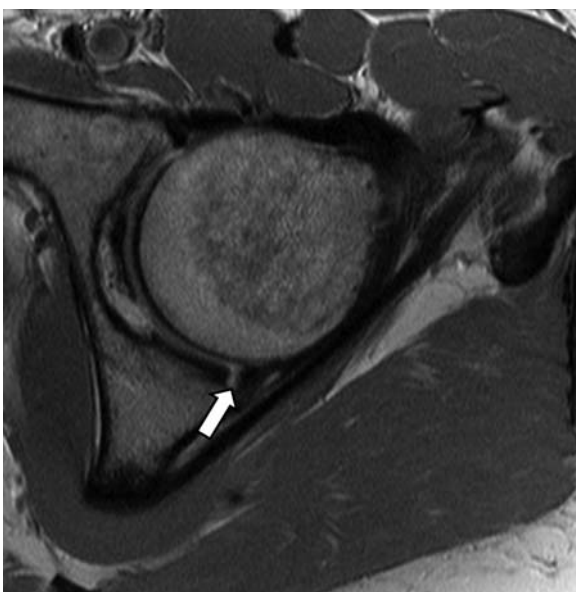


Figure 4 Axial proton-density fast spin-echo image of an asymptomatic volunteer demonstrating the posterior labroligamentous sulcus (white arrow). This should not be confused with labral tear.

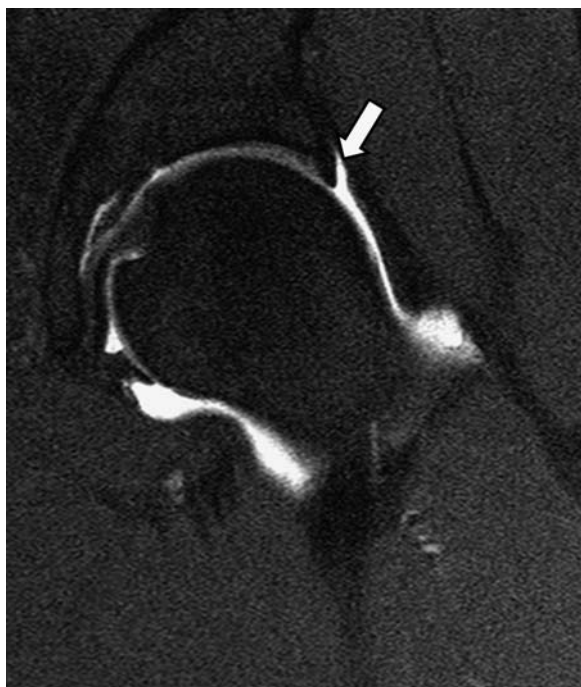


Figure 5 Coronal T1 fat-saturated MR arthrogram image through the midfemoral head following intra-articular gadolinium administration demonstrates a prominent superior perilabral recess formed by a high attachment of the hip capsule to the superior acetabular rim (arrow). This is a common normal finding on MRI.

substantial prevalence of labral hypoplasia in early studies may be related to insufficient resolution to resolve labrum separate from adjacent capsule.

Sublabral recesses or labrocartilaginous clefts (→ Fig. 6a,b), described as a normal undercutting of contrast or fluid along the chondrolabral junction, may be differentiated from tears in that they do not extend greater than half the labral thickness and are wider than deep.^{22,23} The existence of sublabral recesses in the hip is staunchly debated in the

literature with some studies citing no evidence²⁰ and others supporting the existence.^{22,24,25} According to the literature the location of these recesses seems to be the most important factor, with most studies suggesting that they are confined to the anterior and anterior inferior labrum. No normal labral clefts were found beyond the 1 o'clock position (directly anterior defined as 3 o'clock) in two large studies with operative correlation.^{22,25} There remains controversy because one large study with operative correlation demonstrated nearly half of the normal sulci found surgically were located in the anterior superior quadrant.²⁴ Significant discrepancies between these studies may reflect an imperfect gold standard and differences in the surgical definitions of labral tears rather than true differences in the MR appearance.

Ligaments

A layer of thick mechanical fibers encasing the hip joint from the acetabulum to the femoral neck comprise the inelastic hip joint capsule. The fibers are generally oriented in a longitudinal fashion along the axis of the femoral neck with the exception of a thick layer of circumferentially oriented fibers centered at the femoral neck base. These circumferential fibers, known collectively as the zona orbicularis, help secure the femoral head within the acetabular cup. Extracapsular ligaments, named according to their pelvic attachments, add integrity to the hip joint through binding the femur with the adjacent ischium, ilium, and pubis (→ Fig. 7).²⁶ The iliofemoral ligament is the strongest ligament in the human body as a result of the unique twisted attachment at the anterior inferior iliac spine and dual femoral attachment along the intertrochanteric line. This ligament maintains a vertical orientation of the pelvis in the upright position and prevents anterior hip dislocation with extreme extension and external rotation.²⁷ The ischiofemoral ligament fibers course along the superior aspect of the hip joint and blend seamlessly with the crossing fibers of the zona orbicularis of the hip joint capsule.

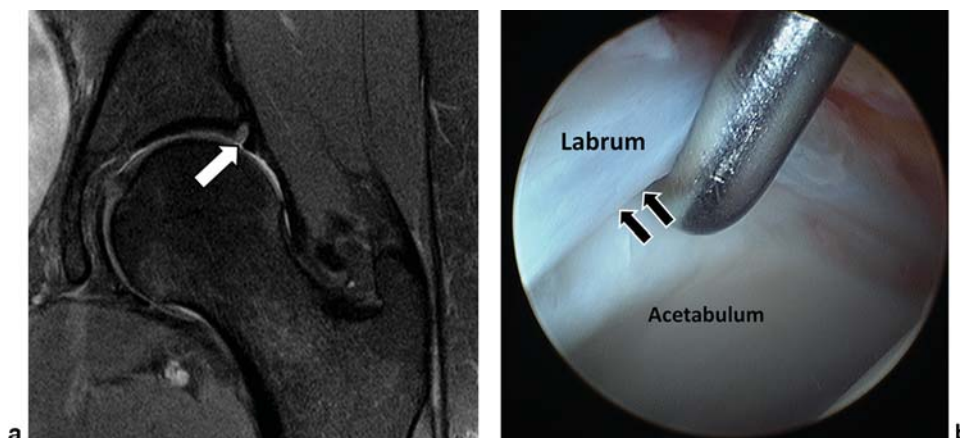


Figure 6 (a) Coronal proton-density fat-saturated MR image through the center of the femoral neck in an asymptomatic patient demonstrates fluid signal interposed between the superior acetabular cartilage and labral base (white arrow) with MRI appearance suggesting labral sulcus rather than a tear. Presence of labral sulci in this area is ardently debated in the literature. (b) Intraoperative arthroscopic image in a different patient, in a similar 12 o'clock position, demonstrating probing of a superior sublabral recess (black arrows), with the arthroscopy probe interposed between the superior labrum and superior acetabular cartilage.

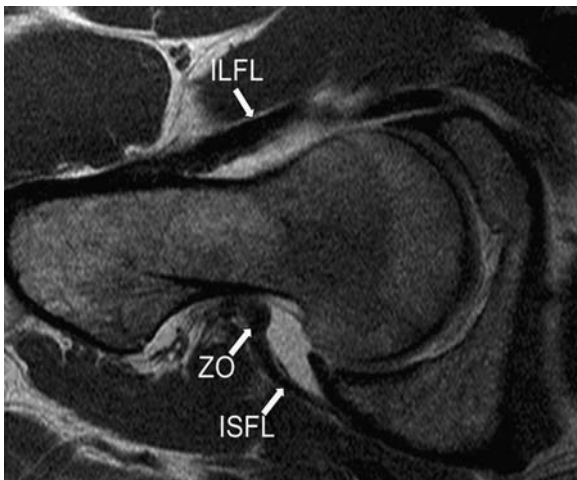


Figure 7 T1-weighted MR arthrogram, axial oblique non-fat-saturated MR image through the level of the midfemoral head demonstrates the uniformly low signal capsular bands defining the anterior and posterior joint capsule. Inferior band of the iliofemoral ligament (ILFL) attaches to the intertrochanteric femoral neck. Ischiofemoral ligament (ISFL) courses laterally from the ischium terminating in a focal thickening representing the zona orbicularis (ZO).

The ischiofemoral ligament prevents excessive motion during internal rotation of the hip. The pubofemoral ligament arises from the superior pubic ramus, extends horizontally to the femoral neck deep to the inferior division of the iliofemoral ligament, and prevents excessive abduction at the hip joint.²⁸

The flat pyramidal shaped ligamentum teres, initially believed to reflect an embryologic remnant with no functional purpose, is now thought to be integral in securing the femoral head articulation with the acetabulum and preventing extreme hip subluxation.²⁹ The ligamentum teres courses from the transverse ligament to the fovea capitis of the femoral head and contains two distinct fascicles originating from the pubic and ischial margins of the acetabular notch (**► Fig. 8a,b**).^{30–32} Although a three-banded structure with medial, anterior, and posterior bands has also been described,³³ the clinical relevance of the bifid versus trifid distinction is questionable because these structures can rarely be differentiated from one another arthroscopically

(**► Fig. 8c**). Congenital absence of the ligamentum teres has also been described, largely in the dysplastic population.³⁴

Plicae

Synovial plicae are embryological remnants or synovial reflections at the articular interfaces that provide structural and functional support to the joint. Two main morphological plical variants, flat and villous, are believed to reflect respective embryologic and acquired plica proliferations: the flat morphology seen exclusively in neonates and the villous seen only in adults.³⁵ Fu et al³⁵ described three plical distributions: labral, ligamentous, and neck plica. The labral plica found interposed between the anterosuperior labrum and iliofemoral ligament is the thickest of the hip plica and most likely to impinge given the close association with the femoroacetabular rim (**► Fig. 9a,b**).³⁶ The ligamentous plica is embedded in the fibrofatty acetabular fossa and runs parallel to the ligamentum teres. Ligamentous plicae are blanketed by a thin layer of synovium and therefore are rarely symptomatic. The neck plica course parallel to the femoral neck and are further subdivided into medial, lateral, and anterior bands or retinacula.³⁷ The lateral retinaculum is found superior to the cortical margin of the femoral neck directly beneath the iliofemoral ligament of the joint capsule, and the medial and anterior retinaculum are located along the inferior margin of the neck. The pectinofoveal fold (**► Fig. 9c,d**) is a prominent synovial reflection along the inferior femoral neck that is reliably seen in 95% of arthrographic studies.^{34,35} Some authors believe the pectinofoveal fold and medial neck plica are synonymous.³⁶ Others believe they are separate structures.³⁵ Although the foveal attachment is uniform between specimens, distal insertion of the pectinofoveal fold may vary with 75% attaching on the joint capsule and 25% attaching directly to the femoral neck.³⁸

Musculature

Flexors

Muscles about the hip are typically classified by function or regional location, but in reality these categories largely overlap. The muscles of the anterior compartment including the rectus femoris, sartorius, iliopsoas, and pectineus act as the primary flexors of the hip (**► Fig. 10a, b**). The iliopsoas

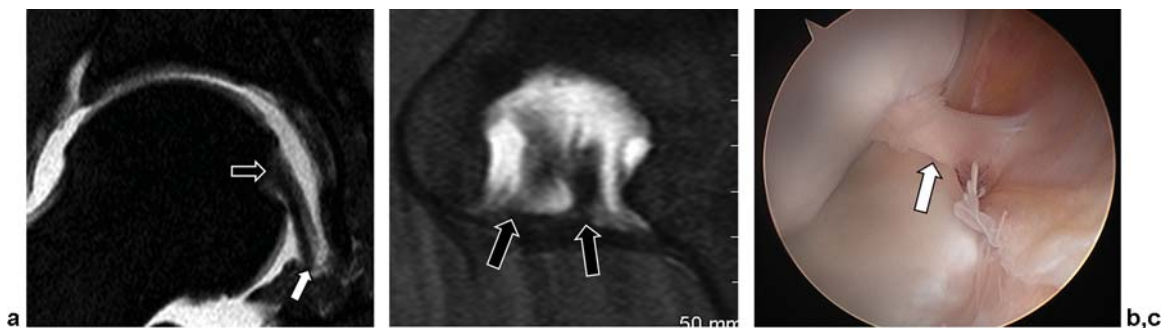


Figure 8 (a) Coronal T1 MR arthrogram fat-saturated image demonstrates the attachments of the ligamentum teres from the fovea capitis (black arrow) to the transverse acetabular ligament (white arrow). (b) T1-weighted sagittal MRI arthrogram fat-saturated image demonstrating the separate ischial and pubic attachments of the ligamentum teres to the transverse ligament (black arrows). (c) Intraoperative arthroscopic image illustrating the normal foveal (left) and acetabular (right) attachments of the ligamentum teres (white arrow).

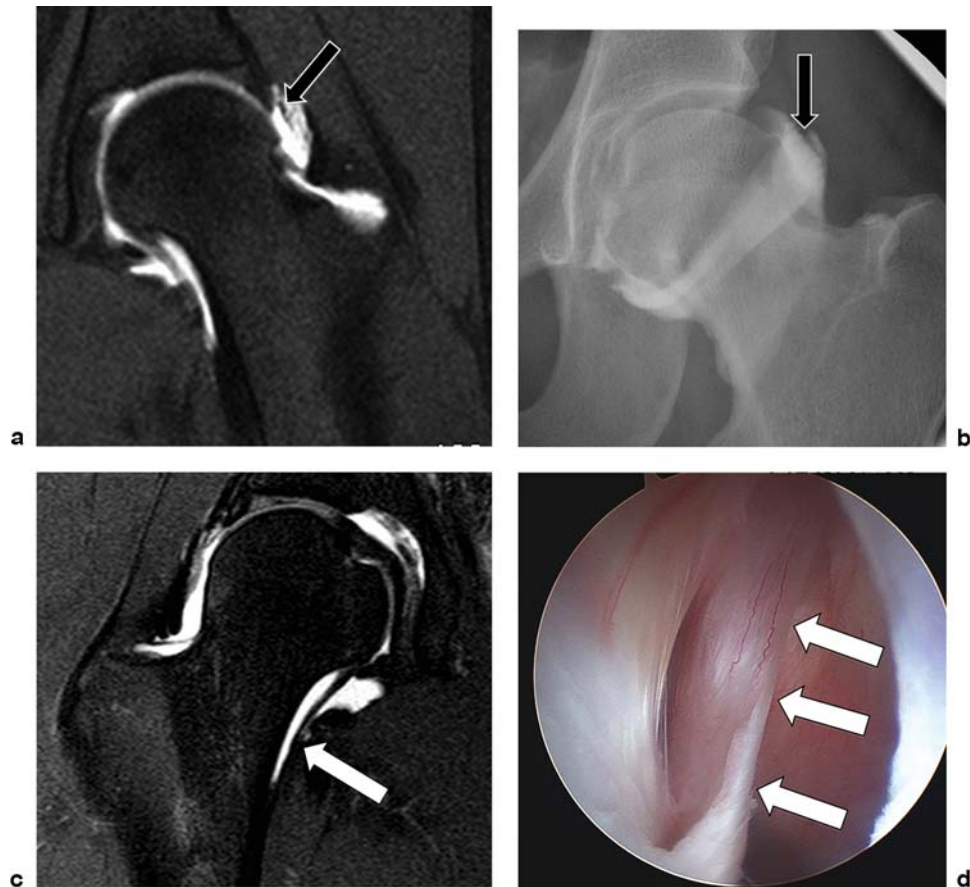


Figure 9 (a) Post-arthrogram T1-weighted fat-saturated coronal MR image demonstrates linear fibrous band in the superior joint recess thought to represent a small labral plica (black arrow). (b) Spot fluoroscopic image from an arthrogram in the same patient shows intra-articular iodine contrast outlining the anterosuperior labral plica (black arrow). (c) T2-weighted fat-saturated coronal MR image following intra-articular gadolinium contrast demonstrates a prominent pectinofoveal fold coursing from the femoral neck/inferior capsule to the fovea capitis (white arrow). (d) Pectinofoveal fold as seen by arthroscopy (white arrows).

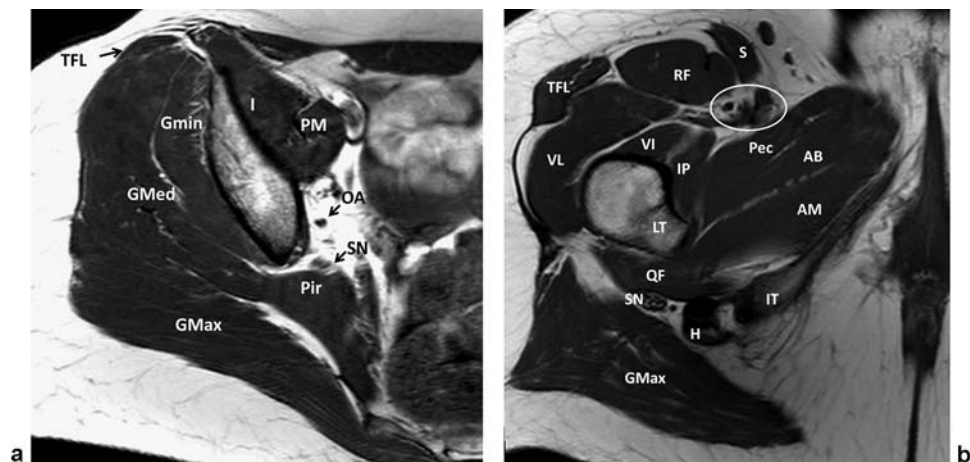


Figure 10 (a) Axial T1-weighted MR image through the level of the ilium demonstrates a normal appearance of the periarticular muscles around the hip joint. I, iliacus; PM, psoas major; TFL, tensor fascia lata; Gmin, gluteus minimus; Gmed, gluteus medius; Gmax, gluteus maximus; Pir, piriformis; OA, obturator artery; SN, sciatic nerve. (b) Axial T1 MRI through the level of the lesser trochanter demonstrates normal muscle anatomy. TFL, tensor fascia lata; RF, rectus femoris; S, sartorius; Pec, pectineus; AB, adductor brevis; AM, adductor magnus; QF, quadratus femoris; Gmax, gluteus maximus; VL, vastus lateralis; VI, vastus interomedialis; IP, iliopsoas; H, hamstring origin; LT, lesser trochanter; IT, ischial tuberosity; SN, sciatic nerve; femoral neurovascular bundle (circle).

muscle is the largest muscle of the anterior compartment and the primary contributor to hip flexion. The muscle is formed by the coalescence of the psoas and iliacus muscles and attaches to the lesser trochanter of the femur. The iliopsoas tendon, unlike other tendons about the hip, is prone to congenital variation. The bifid iliopsoas tendon, well described in the literature, commonly presents with hip snapping syndrome due to motion-related subluxation of the medial and lateral heads.^{39–41} An accessory slip of the iliacus tendon can also be seen in up to 6% of individuals and is represented by a thin fat interface along the medial aspect of the iliopsoas tendon. The femoral nerve may pass between the two myotendinous layers, predisposing to femoral nerve impingement.⁴²

The rectus femoris muscle functions in hip flexion and knee extension and is the only member of the quadriceps muscle group to cross the hip joint. The proximal attachment is bifid with the anterior, or straight, tendon attaching at the anterior inferior iliac spine, and the posterior, or reflected, tendon attaching slightly posterior at the superior acetabular rim. The sartorius muscle originates at the anterior superior iliac spine and attaches distally to the proximal medial surface of the tibia as a component of the pes anserinus. The sartorius functions to flex the hip and internally rotate the thigh. The pectineus muscle arises from the iliopubic ramus and attaches inferior to the iliopsoas muscle tendon on the lesser trochanter. Primary flexors of the hip are innervated by the femoral nerve (L2–L4).

Adductors

Adduction of the hip occurs through contributions from the anteromedial compartment musculature including the adductor magnus, longus and brevis muscles, and the gracilis and pectineus muscles. The oblique and vertical heads of the adductor magnus muscle arise from the inferior pubic ramus and ischial tuberosity, respectively. The gracilis, adductor longus, and adductor brevis muscles originate from the pubic body. The gracilis attaches distally at the proximal medial tibia as part of the pes anserinus. The remaining adductor muscles attach along the linea aspera of the midfemoral shaft. The obturator nerve (L3, L4) innervates the hip adductors with the exception of the vertical head of the adductor magnus muscle, which is supplied by a sciatic nerve branch (L2–L4).

Abductors

The primary abductor muscle group occupies the lateral quadrant and includes the gluteus medius, gluteus minimus, and tensor fascia latae muscles. The gluteus muscles arise from the outer ilium and attach to the greater trochanter of the femur, the gluteus medius at the superoposterior facet, and gluteus minimus deep to the medius fibers on the anterior facet. The tensor fascia latae originates from the anterior iliac spine and attaches to the lateral tibial condyle via the iliotibial tract. Hip abductors, gluteus medius, gluteus minimus, and tensor fascia latae are supplied by the superior gluteal nerve (L4, L5, and S1).

The gluteus maximus muscle originates from the ilium, posterior to the posterior gluteal line, and attaches to the

gluteal tuberosity of the femur and tibial tuberosity via the iliotibial band. The gluteus maximus is innervated by the inferior gluteal nerve (L5, S1, and S2).

Extensors and External Rotators

Extensors and external rotators of the hip are found in the posterior quadrant of the hip and thigh and include the gluteus maximus, piriformis, obturator internus, superior and inferior gemelli, and quadratus femoris. The gluteus maximus is the large superficial muscle that arises from the posterior surface of the ilium and attaches to the lateral tibial condyle via the iliotibial band and is supplied by the inferior gluteal nerve (L5, S1, and S2).

The quadratus femoris arises from the lateral ischial tuberosity and attaches to the quadrate tubercle of the greater trochanter, and it is innervated by the sacral plexus (S1 and S2). The quadratus femoris muscle courses through the ischiofemoral interval and is prone to impingement between these two structures.

The obturator internus originates along the medial curvature of the obturator foramen and joins the superior and inferior gemelli to insert on the lateral greater trochanter. The obturator internus is supplied by the obturator branch (L5 and S1) that also supplies the superior gemellus. The superior and inferior gemelli arise from the ischial spine and ischial tuberosity, respectively. The inferior gemellus is supplied by the nerve to the quadratus femoris (S1 and S2).

The piriformis muscle arises from the anterior lateral sacrum and passes through the greater sciatic notch immediately adjacent to the sciatic nerve and receives innervation by the sacral plexus (S1 and S2). The muscle tendon attaches distally at the superior aspect of the greater trochanter between the iliofemoral ligament anteriorly and gluteus medius tendon posteriorly. Anatomical variation in the piriformis muscle, including duplication of the muscle belly, may predispose to sciatic nerve irritation or impingement.

Extra-articular Structures

Several bursae surround the hip joint and when inflamed may incite significant pain. The iliopsoas bursa, the largest bursa in the body, is bounded by the iliopsoas muscle and tendon anteriorly, the fibrous capsule of the hip posteriorly and femoral vessels medially. It extends from the inguinal ligament to the lesser trochanter and is contiguous with the hip joint in up to 15% of individuals.⁴³ With distension the bursa may take on a horseshoe appearance with lobes extending anteriorly along the sides of the iliopsoas tendon. Cranial extent of the bursa may reach far into the pelvis⁴⁴ and should not be mistaken for a neoplasm.

The greater trochanteric bursa, classically described as a single bursa in the subgluteus maximus region of the lateral thigh, is now known to include multiple distinct bursal compartments that surround the tendinous attachments of the greater trochanter. Nine distinct bursae have been identified around the greater trochanter.⁴⁵ These bursae are discussed in detail elsewhere in this issue. For the purposes of this discussion, three main greater trochanteric bursae are considered: the greater trochanteric, submedius, and

subminimus bursa. The greater trochanteric bursa lies between the tendon of the gluteus maximus and posterior lateral surface of the greater trochanter. The submedius and subminimus bursa lie beneath their respective tendons at the greater trochanteric attachment. Inflammation of these bursae presents as lateral hip pain, which may be confused with lumbar radiculopathy.

Other bursae around the hip include the ischiogluteal, obturator externus, and obturator internus bursae. The ischiogluteal bursa, located deep to the gluteal muscles and posterior to the bony prominence of the ischial tuberosity, when inflamed presents as pain with sitting, a condition known as tailor's or weaver's bottom. The obturator externus bursa, deep to the tendon of the obturator externus muscle, is thought to reflect a potential joint recess from the posterior-inferior hip joint and was found to communicate definitively with the hip joint in up to 6% of patients.⁴⁶ On MR arthrography, care should be taken to differentiate a mildly distended obturator externus bursa from a gadolinium-filled paralabral cyst. The obturator internus bursa, collapsed in normal patients, appears as a boomerang-shaped fluid collection deep to the obturator internus muscle as it turns over the ischium.

Vasculature

Vasculature of the hip is composed of intra- and extracapsular anastomotic rings between the medial and lateral circumflex femoral arteries. Classically the circumflex arteries branch from the profunda femoris and give off deep perforating cervical branches that coalesce into a subsynovial articular ring at the subcapital femoral head. The subsynovial ring gives rise to the lateral epiphyseal arteries. The epiphyseal arteries, along with the medial epiphyseal arteries from the foveal branch of the obturator artery, supply the femoral epiphysis. The delicate cervical perforators along the femoral neck are at risk for disruption in the setting of displaced intracapsular femoral neck fractures. Higher grade displacement of femoral neck fractures (Garden grade 3 and 4) presumes eventual avascular necrosis and is typically treated with the placement of a bipolar hemiprosthesis.

Conventional Radiographic Evaluation of the Hip

Radiography is the initial step in evaluating etiology of hip pain in any patient. Traumatic radiographic evaluation is addressed elsewhere in the issue. Hip morphology can be fully assessed with six views: anteroposterior (AP) pelvis, cross-table lateral, frog-leg lateral, 45 degrees and 90 degrees Dunn views, and false-profile view. All of these views are not performed on any one patient, but some combination is likely preferred by one's local hip surgeon. The proper technique for performing these views and the diagnostic utility of each view are discussed.

Anteroposterior View

The standard AP view of the pelvis should be performed with the patient supine, legs slightly internally rotated, and X-ray beam centered midway between the anterior superior iliac spine and the pubic symphysis (►Fig. 11). X-ray tube-to-film distance should measure 120 cm. Weightbearing views of the pelvis are occasionally performed as an adjunct for assessing pelvic tilt in patients with developmental dysplasia of the hip (DDH).⁴⁷ Appropriate position is ensured when the coccyx and symphysis are centrally aligned and 1 to 2 cm of distance is present between the tip of the coccyx and pubic symphysis. The acetabular teardrop and obturator ring should be easily identified and symmetrical.

The AP view of an individual hip is performed similarly with the X-ray tube centered at the anterior superior iliac spine. Although a dedicated AP view of the unilateral hip improves sensitivity for fractures or bony lesions, AP view of the hip may not accurately portray acetabular version abnormalities. AP view of the pelvis is necessary for optimal assessment of femoroacetabular morphology.⁴⁸

Frog-Leg Lateral

The frog-leg lateral view is performed with the patient in supine position (►Fig. 12). The affected limb is abducted 45 degrees at the hip and flexed 30 to 40 degrees at the knee. The crosshairs of the beam are centered midway between the

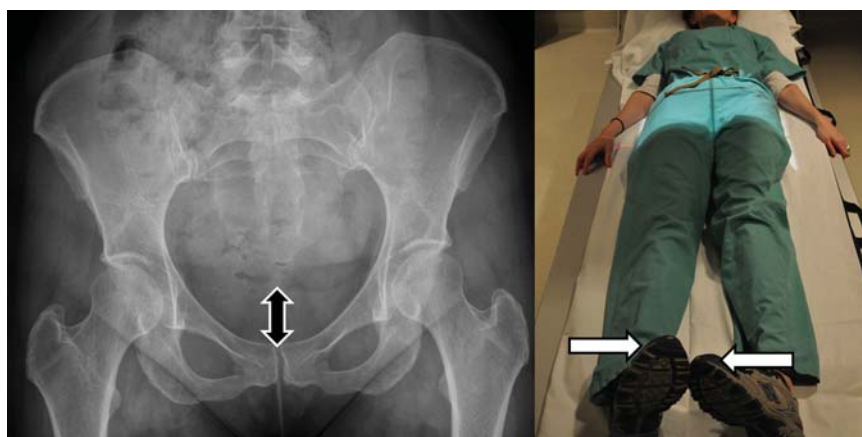


Figure 11 Anteroposterior pelvis. It is essential that the coccyx and the pubic symphysis are aligned and there is 1 to 2 cm distance between the coccyx and the pubic symphysis (black arrow).

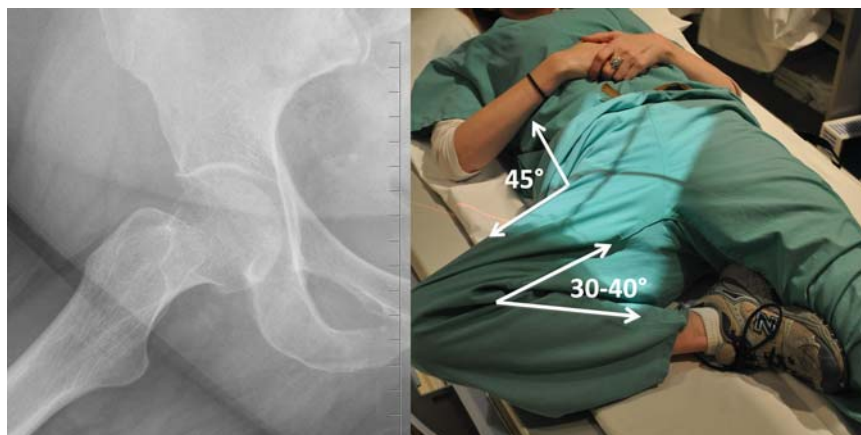


Figure 12 Frog lateral view.

anterior inferior iliac spine and pubic symphysis. The femoral head–neck junction is profiled in a manner that obscures the greater trochanter. This view is used to assess femoral head morphology in the setting of cam-type FAI.

Cross-Table Lateral

The cross-table lateral view is performed with the patient supine and the unaffected hip flexed at 90 degrees out of the beam projection (►Fig. 13). The X-ray beam is centered on the femoral neck, perpendicular to the femoral long axis and at ~102 cm from the film. Proper internal rotation is essential for a diagnostic cross-table lateral view. On a properly positioned examination, the greater trochanter should not overhang the posterior margin and the lesser trochanter should be readily visible.⁴⁹ The cross-table lateral view is performed to assess femoral head neck junction step-off and may provide a better estimate of the femoral version.

The 45- and 90-Degree Dunn Views

The 45-degree and 90-degree Dunn views are performed with the patient supine and the affected hip flexed 45 or 90 degrees with a 20-degree abduction and no hip rotation (►Fig. 14). The X-ray beam is positioned perpendicular to the ASIS and ~102 cm from the film. The Dunn view is superior for assessing the α angle.⁵⁰ The Dunn view was originally described with 90 degrees of hip flexion, but this view is rarely performed now. More commonly the 45-degree Dunn view, or modified Dunn view, is obtained.

False Profile View

The false profile view is performed standing with the affected hip on the cassette (►Fig. 15). The ipsilateral foot is parallel to the cassette with the pelvis rotated 65 degrees from the cassette plane. The false profile view provides a true lateral projection of the femoral head and neck and an oblique view

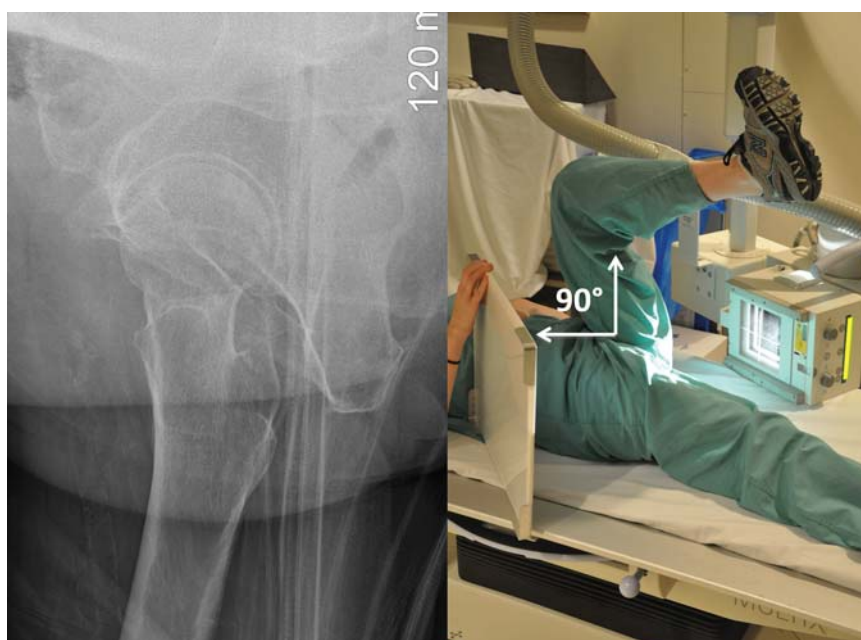


Figure 13 Cross-table lateral view.

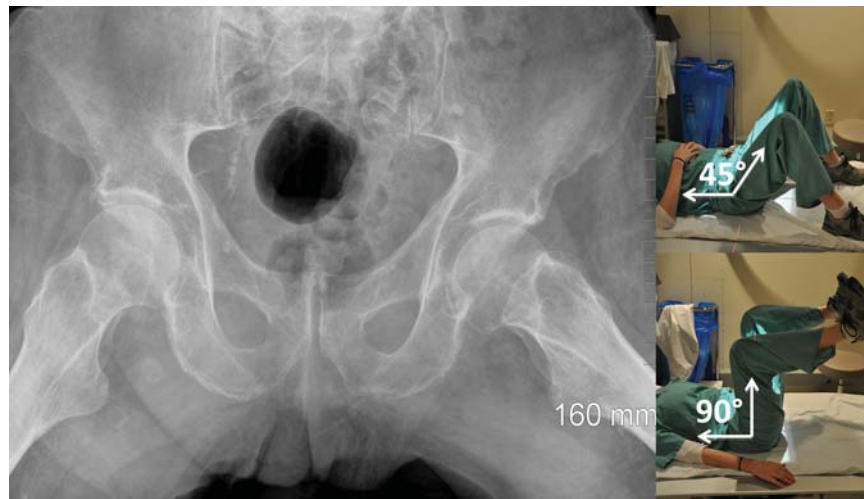


Figure 14 The 45- and 90-degree Dunn views. Radiographic image is of a 45-degree modified Dunn view. The 90-degree Dunn views are not commonly used at this time.

of the acetabulum. Exaggeration or nonvisualization of the lesser trochanter indicates too much internal or external rotation, respectively.⁵¹

MR Imaging

MRI of the hip has become a valuable tool in assessing the multiple potential causes of hip pain. The ability to discern musculotendinous, osseous, cartilaginous, and labral abnormalities has made MRI indispensable in the work-up of the painful hip and groin. MRI of the hip is a challenging joint to image with appropriately high resolution and signal-to-noise ratio. The size of the joint, eccentric location off isocenter, extensive surrounding soft tissues, and the lack of high-

resolution surface coils dedicated to the hip make imaging of the hip difficult.

Several options exist for high-resolution imaging of the hip joint. At our institution, multichannel torso array coils are used for hip imaging. This allows the global assessment of pelvic structures and gross assessment of the contralateral hip while still enabling small field of view (FOV) imaging of the hip in question without the need to exchange coils. Other options include the use of surface flex coils, cardiac coil, and newly available dedicated multichannel hip coils.

For our routine hip protocol we advocate two large 32- to 40-cm FOV sequences, 5- to 7-mm slice thickness, representing a combination of axial and coronal planes and T1-weighted and fluid-sensitive fat-suppressed sequences, for overall assessment

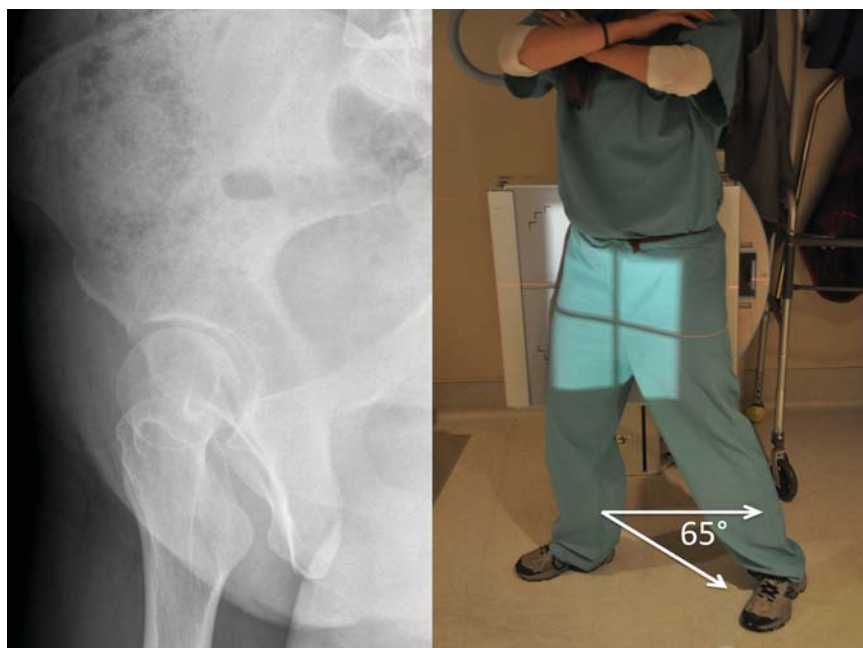


Figure 15 False profile view.

of the pelvis. Dedicated affected hip sequences (16–24 cm FOV, 3-mm slice thickness) afford the resolution capable of discerning abnormalities of the cartilage and labrum. We perform intermediate-weighted proton-density fat-suppressed sequences in all three orthogonal planes, and if hip impingement is a concern, we include an oblique axial T1-weighted image parallel to the long axis of the femoral neck.

Direct MR arthrography (dMRA) utilizes injection of intra-articular dilute gadolinium to allow distension of the hip. This allows the use of high-resolution T1-weighted sequences (16 cm FOV, 3-mm slice thickness) to increase sensitivity and specificity for labral tears and chondral damage.^{20,52–55} We perform T1-weighted fat-suppressed sequences in sagittal and coronal planes with additional fluid-sensitive, intermediate-weighted, fat-suppressed sequences in the coronal plane. Oblique axial T1-weighted and axial three-dimensional (3D) volumetric T1-weighted gradient images round out the protocol. The volumetric acquisition allows reconstruction of two radial sequences, one aligned radially relative to the acetabular labrum and the other designed to tumble around the femoral head neck junction (which we believe aids in assessment of femoral head neck junction bumps). The need for radial images of the labrum is controversial with some advocating radial imaging for improved accuracy⁵⁶ and others demonstrating no additional value.⁵⁷ One of the additional benefits of dMRA is the intra-articular administration of anesthetic, allowing an intra-articular pain generator to be presumed when hip pain is transiently relieved. Additional risk of infection and transiently increased hip pain are downsides to dMRA.

Indirect MR arthrography (iMRA) consists of injection of intravenous gadolinium (0.2 mL/kg) and variable degrees of delay and physical activity to facilitate transsynovial gadolinium excretion into the hip joint and provide greater contrast between the synovial fluid and the labrum and cartilage.^{58,59} Comparable accuracy has been suggested between iMRA and dMRA,^{58,60} although no distension of the joint is afforded by iMRA, and the diagnostic value of the anesthetic arthrogram associated with dMRA is absent. iMRA does not carry the additional risk of septic arthritis and may be logistically favorable in clinical settings where radiologists are not physically able to perform the injection.

There is great interest in MRI techniques to assess the biochemical constituents of cartilage prior to morphological breakdown. The quantitative cartilage assessment techniques measure free water content (T2 mapping) or rely on the fixed negative charge of the building block of the proteoglycan molecule, glycosaminoglycans with delayed gadolinium-enhanced MRI of cartilage (dGEMRIC), T1 ρ (pronounced T1 rho), and²³ sodium (Na) imaging. These techniques are discussed in great detail elsewhere in this issue.

Computed Tomography Imaging

Computed tomography (CT) imaging is widely used for the evaluation of hip and pelvis trauma and is discussed in detail elsewhere in this issue. The ease and speed of acquisition make CT the technique of choice for definitive diagnostic and preoperative imaging of hip and pelvis trauma.

Recently, CT has been advocated as a valuable tool in the assessment of FAI for accuracy of measurements, preoperative planning,³⁵ and even motion simulation.³⁶ The ability of CT to measure the bony margins of the acetabulum accurately and assess morphology of the femoral head–neck junction is profound, and the addition of 3D volume-rendered reconstructions aids the surgeon in preoperative planning.

CT imaging of the pelvis and hip has not been widely standardized for impingement assessment. At our institution, the following protocol is followed. The patients are placed on the CT gantry in the supine position, and care is taken to assure a square pelvis relative to the table. The feet are secured in a neutral toes-up position in a plastic foot binder. We perform whole pelvis 1-mm acquisitions with 2-mm reconstructions in the axial, sagittal, and coronal orthogonal planes. Additional oblique axial 2-mm reconstructions are performed along the long axis of both femoral necks. To calculate the femoral torsion angle, a few additional 3-mm cuts are acquired through the patient's knees. To aid in surgical planning, 3D surface-rendered reconstructions are performed of the entire pelvis to allow detailed morphological evaluation (►Fig. 16).

This protocol allows for routine evaluation of the following measurements: cranial and equatorial acetabular version angle, femoral neck version, femoral torsion, lateral and anterior center edge angles, femoral neck shaft angle, α angle, and femoral head neck offset. These measurements are borrowed from the radiographic literature and have only been partially validated⁶¹ in the surgical literature for CT, but as our experience increases, the confident and accurate reporting of normal and abnormal values, and their implications to patient care, should follow.

Ultrasound Imaging of the Hip

Whereas MRI provides a superior assessment of intraarticular structures such as the labrum⁶² and cartilage, ultrasound is most useful in the dynamic evaluation of the hip. This feature



Figure 16 Computed tomography three-dimensional reconstruction of the hip and pelvis offers a global view of bony hip anatomy and is often used by hip surgeons for preoperative planning.



Figure 17 Imaging along the femoral neck long axis with a linear high frequency 12-mHz transducer demonstrates a normal anterior joint recess (white arrow) with negligible joint fluid visible over the convexity of the femoral head.

is particularly important when characterizing a snapping hip or guiding an intervention such as a therapeutic steroid injection. Additional advantages include the relatively low cost, wide availability, and absence of ionizing radiation. Knowledge of sonographic anatomy reinforces and rounds out the radiologist's understanding of the hip and surrounding structures.

The hip is best evaluated using a high-frequency transducer. The anterior hip joint is evaluated with the patient supine and the transducer oriented longitudinally along the long axis of the femoral neck. From this position, the femoral head, acetabular labrum, and anterior joint recess are visible (→ **Fig. 17**). This view is useful in evaluating the joint capsule ligaments, which appear as slightly hyperechoic structures measuring 2 to 4 mm in thickness⁶³ and superior in assessing for the presence of joint effusion. The thickness of the fluid layer along the anterior recess can be used to differentiate pathologic and physiologic joint fluid. Ultrasound is particularly useful in evaluating for the presence or absence of hip effusion, distension of the trochanteric bursae, and pathology at the tendinous insertions of the gluteal, adductor, and hamstring tendons. Evaluation of the hip labrum by ultrasound is limited with a sensitivity <50%.⁶⁴

Radiographic Assessment of the Hip: Pertinent Lines and Measurements (→ **Table 1**)

Pelvic and hip trauma is covered elsewhere in this issue. Radiographs may also be used in determining the early evidence of hip osteoarthritis. The smallest distance between the femoral head and the acetabulum is termed the *joint space width* and should normally measure 3 to 5 mm.⁶⁵ Narrowing of the joint space width or asymmetric joint space narrowing are often the first sign of osteoarthritis⁴⁹.

Hip measurements are used to assess for a variety of disorders. By far the most common is DDH and FAI. An explosion of measurements in the recent literature attempt to provide a more sophisticated preoperative assessment of these conditions and are being utilized with increasing frequency by specialized hip surgeons. Although many of these measurements can be made on hip or pelvic radiographs, this would not be considered a standard in routine assessment of the hip.

Acetabular Coverage Measurements

Acetabular depth as determined on AP view is assessed through evaluation of the medial margin of the femoral head and acetabulum with respect to the ilioischial line. Coxa profunda is present when the floor of the acetabular fossa is in line with the ilioischial line; acetabular protrusion occurs when the medial cortex of the femoral head overlaps the ilioischial line. Abnormal acetabular depth from any cause (congenital, posttraumatic, inflammatory arthropathies, soft bone diseases) leads to femoral head overcoverage and acceleration of hip joint degeneration.

The acetabulum normally covers ~75% of the femoral head. Abnormal acetabular undercoverage and overcoverage, seen in hip dysplasia and pincer impingement, respectively, can be quantitated by the lateral and anterior center edge angle, femoral head extrusion index, and acetabular depth.

Lateral Center Edge Angle

The lateral center edge (CE) angle of Wiberg, measured on the AP pelvic radiograph, estimates acetabular overcoverage and undercoverage of the femoral head. The lateral CE angle is formed by the angle of two lines, the first through the center of the femoral head perpendicular to the pelvic horizontal or teardrop line, and the second through the lateral margin of the acetabulum. In 1990, Ogata et al proposed a revised CE angle measurement, or Ogata's angle, which utilizes the sclerotic or condensed acetabular roof (sourcil) as the lateral margin of the superior acetabular cup. This proposal was a response to Ogata's observation that acetabular retroversion overestimated lateral CE angle in patients with DDH.^{66,67}

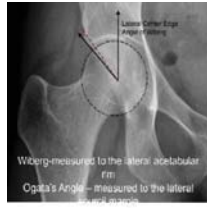




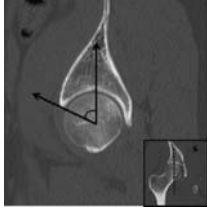





Femoral Head Extrusion Index

Femoral head extrusion index (FHEI) is an alternative, somewhat more cumbersome, estimation of acetabular coverage. To calculate the FHEI, first determine the length of the femoral head that lies beyond the confines of the acetabulum (A), divide by the total horizontal width of femoral head (B), and multiply by 100 to obtain a percentage ($[A/B] \times 100$). A value >25% is considered abnormal.⁴⁸ Jacobsen et al⁶⁸ measures the FHEI slightly differently by using the medial femoral cortex to lateral acetabular rim distance divided by the diameter of the femoral head, a measurement also referred to as femoral head coverage.⁶⁹ In this instance, abnormal values would be <75%.

Anterior Center Edge Angle

A false profile view or sagittal cross-sectional image is used to evaluate anterior acetabular coverage. Anterior CE angle is measured by a line connecting the central femoral head and

Table 1 Common measurements important to hip surgeons

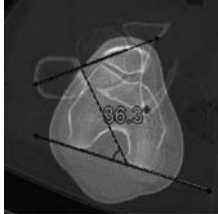
Measurement	Normal	Pathologic	Measurement technique CR	Measurement technique CT
Lateral center edge angle ^{66,96}	25–40 degrees (borderline: 20–25 degrees)	<20 degrees >40 degrees		
Femoral head extrusion index	<25% ⁶⁸	>25% ⁷		
Femoral head coverage ⁶⁹	>75%	<75%		
Anterior center edge angle ⁵¹	20–40 degrees	>40 degrees <20 degrees		Not well validated 
Acetabular quotient (depth ratio) ^{68,69}	>250	<250		
Tonnis angle, (sourcil angle, Acetabular roof obliquity) ⁷⁴	0–10 degrees	<0 degrees >10 degrees		Sourcil margins are not clearly defined on cross-sectional imaging
Sharps angle (acetabular inclination) ⁷¹	<45 degrees	>45 degrees		

(Continued)

Table 1 (Continued)

Measurement	Normal	Pathologic	Measurement technique CR	Measurement technique CT
Equatorial acetabular version ^{72,73,97}	13–20 degrees	<0 degrees	N/A	
Cranial acetabular version ^{61,72,73}	5–8 degrees	<0 degrees	NA	
α Angle ⁸⁰	<50 degrees	>50 degrees		
Femoral head–neck offset ⁴⁹ and ratio ⁸³	>9 mm or >0.18 ratio	<9 mm or <0.18 ratio		
Femoral neck shaft angle ^{61,87,98,99}	125–135 degrees	<120 degrees >140 degrees		
Femoral neck version angle ¹⁰⁰	5–25 degrees	<5 degrees >25 degrees	NA	

Table 1 (Continued)

Measurement	Normal	Pathologic	Measurement technique CR	Measurement technique CT
Femoral torsion angle ⁸⁸	10–20 degrees	<10 degrees >20 degrees	NA	

Abbreviations: CT, computed tomography; CR, conventional radiography; NA, not applicable.

*no studies have yet defined a minimum normal for FHEI

anterior acetabular rim with a line perpendicular to the horizontal axis on cross-sectional sagittal or parallel to the femoral neck on false profile view. The CT and radiographic measurements described earlier are not analogous, and, in our experience, the CT equivalent is typically significantly greater. The CT assessment of anterior acetabular coverage still needs validation and should be interpreted with caution.

Acetabular Quotient

Acetabular quotient (acetabular depth ratio) evaluates the depth of the acetabular cup, and it is determined by the ratio of the acetabular width (distance from the inferior teardrop to the lateral rim) and the depth (perpendicular distance from the midpoint of the width line to the acetabular dome). The quotient is calculated with the equation acetabular depth/acetabular width $\times 1000$ ⁶⁹ with cut-off values for hip dysplasia at 250.⁶⁸



Figure 18 Anteroposterior radiograph of the pelvis demonstrates the orientation of the anterior and posterior acetabular wall in a normally anteverted patient. Anterior acetabular wall (dotted line) is continuous with the superior pubic ramus. Posterior acetabular wall (dashed line) blends with the ischium.

Acetabular Inclination

The acetabular inclination is estimated using the Tonnis angle and Sharps angle. The Tonnis angle, also known as the sourcil angle or acetabular roof obliquity,^{70,74} estimates the inclination angle of the weightbearing acetabulum. The angle apex lies at the medial margin of the sclerotic sourcil with limbs to the lateral sourcil margin and along the horizontal axis of the pelvis. The Sharps angle provides an estimation of overall acetabular inclination and is formed by connecting a horizontal line from the distal teardrop and oblique line to the superolateral acetabular rim.⁷¹ Steepening of the inclination angle is seen in patients with developmental dysplasia of the hip.

Acetabular Version

Orientation of the acetabulum relative to the horizontal axis of the pelvis defines the acetabular version. Using axial CT images, the acetabular version is formed by a line connecting the anterior and posterior margins of the acetabulum and a line paralleling the vertical axis of the pelvis. The version can be measured at both equatorial and cranial axes of the acetabulum. The acetabular cup normally opens anteriorly with a version angle of 15 to 20 degrees at the equatorial center of the acetabulum. Anteversion angle decreases more cranially, ultimately nearing the perpendicular pelvic axis (0 degrees) at the acetabular roof (normal cranial acetabular version 5 degrees \pm 5 degrees).^{72,73} Abnormalities in acetabular anteversion have been associated with hip osteoarthritis and pincer-type FAI.^{74–76} Excessive anteversion has been noted with developmental dysplasia of the hip,^{77,78} but discrete measurements of excessive anteversion have not been well validated in the literature. It has been our experience that a subset of patients is unstable anterolaterally related to excessive anteversion (or focal acetabular dysplasia resulting in excessive anteversion measurements), but we have yet to arrive at a discrete abnormal measurement.

Gross assessment of acetabular version can be made radiographically but requires an understanding of the radiographic acetabular anatomy (—Fig. 18). In a normal anteverted acetabulum, the anterior and posterior walls meet at the superolateral edge of the acetabulum. When the acetabulum is retroverted the anterior wall lateralizes and a “cross-over”

sign is apparent with medialization of the superoposterior acetabular wall. Differences in pelvic tilt and beam angulation can easily confound this appearance, and proper positioning should be verified prior to assessing this parameter. True retroversion of the acetabulum can contribute to projection of the ischial spine into the pelvis, making it more apparent on the AP radiographic view. This has been described as the ischial spine sign.⁷⁹

Femoral Head Morphology Assessment

A narrow neck relative to the spherical femoral head allows for the wide range of rotator and flexion motions at the hip joint. Femoral head neck junction bumps seen in the setting of cam-type FAI limit range of motion at the hip and predispose to labral injury and premature osteoarthritis. These bumps occur most commonly at the anterosuperior head-neck junction and are estimated using the α angle and femoral head-neck offset and offset ratio.

The α Angle

The α angle is formed by a line from the center of the femoral head down the axis of the femoral neck and a second line connecting the center of the femoral head with the site at which the femoral neck bump exits the sphericity of the femoral head.⁶¹ An α angle measurement >50 to 55 degrees can be associated with abnormal femoral/acetabular collision with motion.⁸⁰ This angle is measured on CT or MRI using an axial oblique cross-sectional image oriented parallel to the long axis of the femoral neck. However, several studies have shown greater accuracy with radiographic measurements.^{50,81} Although often measured on cross-table lateral views, the 45-degree Dunn view has proven most sensitive and specific for the evaluation of α angles in the hip.^{50,82}

Femoral Head-Neck Offset

The femoral head-neck offset, measured on the same projection or cross-sectional image as the α angle, assesses the adequacy of the femoral waist. The distance between the most anterior aspect of the femoral head and exit site of the α angle (measured using lines parallel to the axis of the femoral neck) is termed the *offset value*. This value can produce a ratio by dividing by the femoral head diameter, with a value <0.18 considered abnormal.⁸³

Femoral Neck and Shaft Orientation

Femoral Neck Shaft Angle

The femoral neck shaft angle, measured on coronal cross-sectional or AP radiograph, is formed by lines through the central medullary cavity of the femoral neck and femoral shaft with apex at the intertrochanteric line (normal: 120 – 140). The terms *coxa valga* and *coxa vera* are used to describe femoral neck shaft angles that are abnormally high and low, respectively.

Femoral Neck Version

Distinction should be made between the femoral torsion angle and the femoral neck version angle, the latter of which

measures the angle of the femoral neck relative to the horizontal axis of the pelvis. Abnormal femoral torsion begets abnormal neck version at the acetabulum explaining the interchangeable use of these terms *femoral torsion* and *femoral neck anteversion* in the literature. The femoral neck version angle measures the anteversion or retroversion of the femoral neck relative to the horizontal axis of the pelvis. This measurement depends on internal and external rotation of the extremity, and it is standardized by securing the feet in neutral toes-up position in a plastic foot binder. Abnormalities in the femoral version predispose to a wide range of orthopedic abnormalities including premature osteoarthritis, hip dysplasia, slipped capital femoral epiphyses, labral tears, and ischiofemoral impingement.^{84–86} At our institution in an attempt to minimize technical difficulties in obtaining these measurements, fusion CT images are utilized. Femoral neck version angle is measured by fusing an axial image through the central femoral head and the base of the femoral neck at the lesser trochanter. A line through the femoral neck axis (central femoral head and central femoral shaft at the lesser trochanter) and a line across the horizontal axis of the pelvis form the femoral version angle. Retroversion of the femoral neck relative to the horizontal axis is abnormal.

Femoral Torsion

Femoral torsion refers to the relative rotation between the neck and the shaft of the femur as measured by the angle between the femoral neck and the horizontal axis of femoral condyles. To improve measurement accuracy, at our institution we fuse three axial CT images: the central femoral head, the lesser trochanter of the femur, and the distal femoral condyles. Image fusion through the central femoral head and lesser trochanter allows accurate measurement of the femoral neck axis, which is then measured against the axis of the posterior femoral condyles to create the femoral torsion angle. There is significant variability in normal torsion angles presented in the literature, suggested by some to reflect evolutionary differences between geographically and ethnically different human populations. The most widely accepted normal range measures 10 to 20 degrees.^{87–93} Elevated torsion angles are seen in patients with developmental hip dysplasia and FAI.^{89,94} Abnormalities in femoral torsion are important to recognize because they may predispose to early osteoarthritis, patellar maltracking, or FAI.^{74,89,95}

Conclusion

Hip imaging and assessment of hip disorders is one of the most rapidly growing subsets of musculoskeletal radiology. A detailed knowledge of normal hip anatomy, hip imaging options, and normal and abnormal spatial relationships between the femoral head, acetabulum, and femoral axis is becoming a crucial component of the radiologist's knowledge base. The current attitudes on FAI and developmental dysplasia, and the push to implement early and aggressive treatment of these conditions, has increased demand for sophisticated CT, MR, and radiographic measurements and expanded the role of radiologists in the realm of hip surgery.

References

- 1 Brückl R, Tönnis D. The growth of the juvenile hip joint. A planimetric study of x-ray films (author's transl) [in German]. *Arch Orthop Trauma Surg* 1979;93(2):149–159
- 2 Wierusz-Kozłowska M, Ziemiański A, Kruczyński J, Borkowski W. Development of the normal infantile hip joints assessed by MRI [in Polish]. *Chir Narządów Ruchu Ortop Pol* 2000;65(1):25–32
- 3 Wyler A, Bousson V, Bergot C, et al. Comparison of MR-arthrography and CT-arthrography in hyaline cartilage-thickness measurement in radiographically normal cadaver hips with anatomy as gold standard. *Osteoarthritis Cartilage* 2009;17(1):19–25
- 4 Dietrich TJ, Suter A, Pfirrmann CW, Dora C, Fucentese SF, Zanetti M. Supraacetabular fossa (pseudodeflect of acetabular cartilage): frequency at MR arthrography and comparison of findings at MR arthrography and arthroscopy. *Radiology* 2012;263(2):484–491
- 5 Hergan K, Oser W, Moriggl B. Acetabular ossicles: normal variant or disease entity? *Eur Radiol* 2000;10(4):624–628
- 6 Arho AO. Accessory bones of extremities in roentgen picture. *Duodecim* 1940;56:399–410
- 7 Martinez AE, Li SM, Ganz R, Beck M. Os acetabuli in femoroacetabular impingement: stress fracture or unfused secondary ossification centre of the acetabular rim? *Hip Int* 2006;16(4):281–286
- 8 Kassarian A, Yoon LS, Belzile E, Connolly SA, Millis MB, Palmer WE. Triad of MR arthrographic findings in patients with cam-type femoroacetabular impingement. *Radiology* 2005;236(2):588–592
- 9 Klaue K, Durnin CW, Ganz R. The acetabular rim syndrome. A clinical presentation of dysplasia of the hip. *J Bone Joint Surg Br* 1991;73(3):423–429
- 10 Cooke WR, Gill HS, Murray DW, Ostlere SJ. Discrete mineralisation of the acetabular labrum: a novel marker of femoroacetabular impingement? *Br J Radiol* 2013;86(1021):20120182
- 11 Smith MV, Panchal HB, Ruberte Thiele RA, Sekiya JK. Effect of acetabular labrum tears on hip stability and labral strain in a joint compression model. *Am J Sports Med* 2011;39(Suppl):1035–110S
- 12 Edwards DJ, Lomas D, Villar RN. Diagnosis of the painful hip by magnetic resonance imaging and arthroscopy. *J Bone Joint Surg Br* 1995;77(3):374–376
- 13 Petersilge CA, Haque MA, Petersilge WJ, Lewin JS, Lieberman JM, Buly R. Acetabular labral tears: evaluation with MR arthrography. *Radiology* 1996;200(1):231–235
- 14 Cotten A, Boutry N, Demondion X, et al. Acetabular labrum: MRI in asymptomatic volunteers. *J Comput Assist Tomogr* 1998;22(1):1–7
- 15 Gerhardt M, Johnson K, Atkinson R, et al. Characterisation and classification of the neural anatomy in the human hip joint. *Hip Int* 2012;22(1):75–81
- 16 Petersilge C. Imaging of the acetabular labrum. *Magn Reson Imaging Clin N Am* 2005;13(4):641–652, vi
- 17 Groh MM, Herrera J. A comprehensive review of hip labral tears. *Curr Rev Musculoskelet Med* 2009;2(2):105–117
- 18 Lecouvet FE, Vande Berg BC, Malghem J, et al. MR imaging of the acetabular labrum: variations in 200 asymptomatic hips. *AJR Am J Roentgenol* 1996;167(4):1025–1028
- 19 Hodler J, Yu JS, Goodwin D, Haghghi P, Trudell D, Resnick D. MR arthrography of the hip: improved imaging of the acetabular labrum with histologic correlation in cadavers. *AJR Am J Roentgenol* 1995;165(4):887–891
- 20 Czerny C, Hofmann S, Urban M, et al. MR arthrography of the adult acetabular capsular-labral complex: correlation with surgery and anatomy. *AJR Am J Roentgenol* 1999;173(2):345–349
- 21 Aydingöz U, Oztürk MH. MR imaging of the acetabular labrum: a comparative study of both hips in 180 asymptomatic volunteers. *Eur Radiol* 2001;11(4):567–574
- 22 Studler U, Kalberer F, Leunig M, et al. MR arthrography of the hip: differentiation between an anterior sublabral recess as a normal variant and a labral tear. *Radiology* 2008;249(3):947–954
- 23 DuBois DF, Omar IM. MR imaging of the hip: normal anatomic variants and imaging pitfalls. *Magn Reson Imaging Clin N Am* 2010;18(4):663–674
- 24 Saddik D, Troupis J, Tirman P, O'Donnell J, Howells R. Prevalence and location of acetabular sublabral sulci at hip arthroscopy with retrospective MRI review. *AJR Am J Roentgenol* 2006;187(5):W507–W511
- 25 Dinauer PA, Murphy KP, Carroll JF. Sublabral sulcus at the posteroinferior acetabulum: a potential pitfall in MR arthrography diagnosis of acetabular labral tears. *AJR Am J Roentgenol* 2004;183(6):1745–1753
- 26 Smith MV, Costic RS, Allaire R, Schilling PL, Sekiya JK. A biomechanical analysis of the soft tissue and osseous constraints of the hip joint. *Knee Surg Sports Traumatol Arthrosc* 2012; October 30 (Epub ahead of print)
- 27 Fuss FK, Bacher A. New aspects of the morphology and function of the human hip joint ligaments. *Am J Anat* 1991;192(1):1–13
- 28 Wagner FV, Negrão JR, Campos J, et al. Capsular ligaments of the hip: anatomic, histologic, and positional study in cadaveric specimens with MR arthrography. *Radiology* 2012;263(1):189–198
- 29 Martin RL, Kivlan BR, Clemente FR. A cadaveric model for ligamentum teres function: a pilot study. *Knee Surg Sports Traumatol Arthrosc* 2012; November 2 (Epub ahead of print)
- 30 Keene GS, Villar RN. Arthroscopic anatomy of the hip: an in vivo study. *Arthroscopy* 1994;10(4):392–399
- 31 Gray AJ, Villar RN. The ligamentum teres of the hip: an arthroscopic classification of its pathology. *Arthroscopy* 1997;13(5):575–578
- 32 Armfield DR, Towers JD, Robertson DD. Radiographic and MR imaging of the athletic hip. *Clin Sports Med* 2006;25(2):211–239, viii
- 33 Demange M. Influence of the femoral head ligament on hip mechanical function. *Acta Ortop Bras.* 2007;15(4):187–190
- 34 Remes V, Tervahartiala P, Helenius I, Peltonen J. Magnetic resonance imaging analysis of hip joint development in patients with diastrophic dysplasia. *J Pediatr Orthop* 2002;22(2):212–216
- 35 Fu Z, Peng M, Peng Q. Anatomical study of the synovial plicae of the hip joint. *Clin Anat* 1997;10(4):235–238
- 36 Bencardino JT, Kassarian A, Vieira RL, Schwartz R, Mellado JM, Kocher M. Synovial plicae of the hip: evaluation using MR arthrography in patients with hip pain. *Skeletal Radiol* 2011;40(4):415–421
- 37 Bartoníček J. Weitbrecht's retinacula of the hip joint [in Czech]. *Acta Chir Orthop Traumatol Cech* 1990;57(5):385–391
- 38 Blankenbaker DG, Davis KW, De Smet AA, Keene JS. MRI appearance of the pectinofoveal fold. *AJR Am J Roentgenol* 2009;192(1):93–95
- 39 Tatu L, Parratte B, Vuillier F, Diop M, Monnier G. Descriptive anatomy of the femoral portion of the iliopsoas muscle. Anatomical basis of anterior snapping of the hip. *Surg Radiol Anat* 2001;23(6):371–374
- 40 Guillin R, Cardinal E, Bureau NJ. Sonographic anatomy and dynamic study of the normal iliopsoas musculotendinous junction. *Eur Radiol* 2009;19(4):995–1001
- 41 Shu B, Safran MR. Case report: Bifid iliopsoas tendon causing refractory internal snapping hip. *Clin Orthop Relat Res* 2011;469(1):289–293
- 42 Spratt JD, Logan BM, Abrahams PH. Variant slips of psoas and iliacus muscles, with splitting of the femoral nerve. *Clin Anat* 1996;9(6):401–404
- 43 Chandler S. The iliopsoas bursa in man. *Anat Rec* 1934;36:235–240
- 44 Varma DG, Richli WR, Charnsangavej C, Samuels BI, Kim EE, Wallace S. MR appearance of the distended iliopsoas bursa. *AJR Am J Roentgenol* 1991;156(5):1025–1028
- 45 Woodley SJ, Mercer SR, Nicholson HD. Morphology of the bursa associated with the greater trochanter of the femur. *J Bone Joint Surg Am* 2008;90(2):284–294

- 46 Kassirjian A, Llopis E, Schwartz RB, Bencardino JT. Obturator externus bursa: prevalence of communication with the hip joint and associated intra-articular findings in 200 consecutive hip MR arthrograms. *Eur Radiol* 2009;19(11):2779–2782
- 47 Troelsen A, Jacobsen S, Rømer L, Søballe K. Weightbearing anteroposterior pelvic radiographs are recommended in DDH assessment. *Clin Orthop Relat Res* 2008;466(4):813–819
- 48 Tannast M, Siebenrock KA, Anderson SE. Femoroacetabular impingement: radiographic diagnosis—what the radiologist should know. *AJR Am J Roentgenol* 2007;188(6):1540–1552
- 49 Clohisy JC, Carlisle JC, Beaulé PE, et al. A systematic approach to the plain radiographic evaluation of the young adult hip. *J Bone Joint Surg Am* 2008;90(Suppl 4):47–66
- 50 Barton C, Salineros MJ, Rakhra KS, Beaulé PE. Validity of the alpha angle measurement on plain radiographs in the evaluation of cam-type femoroacetabular impingement. *Clin Orthop Relat Res* 2011;469(2):464–469
- 51 Lequesne M, de SEZE. False profile of the pelvis. A new radiographic incidence for the study of the hip. Its use in dysplasias and different coxopathies. [in French]. *Rev Rhum Mal Osteoartic* 1961;28:643–652
- 52 Chan YS, Lien LC, Hsu HL, et al. Evaluating hip labral tears using magnetic resonance arthrography: a prospective study comparing hip arthroscopy and magnetic resonance arthrography diagnosis. *Arthroscopy* 2005;21(10):1250
- 53 Czerny C, Hofmann S, Neuhold A, et al. Lesions of the acetabular labrum: accuracy of MR imaging and MR arthrography in detection and staging. *Radiology* 1996;200(1):225–230
- 54 Leunig M, Werlen S, Ungersböck A, Ito K, Ganz R. Evaluation of the acetabular labrum by MR arthrography. *J Bone Joint Surg Br* 1997;79(2):230–234
- 55 Toomayan GA, Holman WR, Major NM, Kozlowski SM, Vail TP. Sensitivity of MR arthrography in the evaluation of acetabular labral tears. *AJR Am J Roentgenol* 2006;186(2):449–453
- 56 Plötz GM, Brossmann J, von Knoch M, Muhle C, Heller M, Hassenpflug J. Magnetic resonance arthrography of the acetabular labrum: value of radial reconstructions. *Arch Orthop Trauma Surg* 2001;121(8):450–457
- 57 Yoon LS, Palmer WE, Kassirjian A. Evaluation of radial-sequence imaging in detecting acetabular labral tears at hip MR arthrography. *Skeletal Radiol* 2007;36(11):1029–1033
- 58 Zlatkin MB, Pevsner D, Sanders TG, Hancock CR, Ceballos CE, Herrera MF. Acetabular labral tears and cartilage lesions of the hip: indirect MR arthrographic correlation with arthroscopy—a preliminary study. *AJR Am J Roentgenol* 2010;194(3):709–714
- 59 Vahlensieck M, Peterfy CG, Wischer T, et al. Indirect MR arthrography: optimization and clinical applications. *Radiology* 1996;200(1):249–254
- 60 Pozzi G, Stradiotti P, Parra CG, Zagra L, Sironi S, Zerbi A. Femoroacetabular impingement: can indirect MR arthrography be considered a valid method to detect endoarticular damage? A preliminary study. *Hip Int* 2009;19(4):386–391
- 61 Dolan MM, Heyworth BE, Bedi A, Duke G, Kelly BT. CT reveals a high incidence of osseous abnormalities in hips with labral tears. *Clin Orthop Relat Res* 2011;469(3):831–838
- 62 Jin W, Kim KI, Rhyu KH, et al. Sonographic evaluation of anterosuperior hip labral tears with magnetic resonance arthrographic and surgical correlation. *J Ultrasound Med* 2012;31(3):439–447
- 63 Robben SG, Lequin MH, Diepstraten AF, den Hollander JC, Entius CA, Meradji M. Anterior joint capsule of the normal hip and in children with transient synovitis: US study with anatomic and histologic correlation. *Radiology* 1999;210(2):499–507
- 64 Troelsen A, Mechlenburg I, Gelineck J, Bolvig L, Jacobsen S, Søballe K. What is the role of clinical tests and ultrasound in acetabular labral tear diagnostics? *Acta Orthop* 2009;80(3):314–318
- 65 Fredensborg N, Nilsson BE. The joint space in normal hip radiographs. *Radiology* 1978;126(2):325–326
- 66 Ogata S, Moriya H, Tsuchiya K, Akita T, Kamegaya M, Someya M. Acetabular cover in congenital dislocation of the hip. *J Bone Joint Surg Br* 1990;72(2):190–196
- 67 Omeroglu H, Biçimoglu A, Ağuş H, Tümer Y. Measurement of center-edge angle in developmental dysplasia of the hip: a comparison of two methods in patients under 20 years of age. *Skeletal Radiol* 2002;31(1):25–29
- 68 Jacobsen S, Sonne-Holm S, Søballe K, Gebuhr P, Lund B. Hip dysplasia and osteoarthritis: a survey of 4151 subjects from the Osteoarthritis Substudy of the Copenhagen City Heart Study. *Acta Orthop* 2005;76(2):149–158
- 69 Pedersen DR, Lamb CA, Dolan LA, Ralston HM, Weinstein SL, Morcuende JA. Radiographic measurements in developmental dysplasia of the hip: reliability and validity of a digitizing program. *J Pediatr Orthop* 2004;24(2):156–160
- 70 Umer M, Sepah YJ, Asif S, Azam I, Jawad MU. Acetabular morphology and prevalence of hip dysplasia in the South Asian population. *Orthop Rev (Pavia)* 2009;1(1):e10
- 71 Sharp I. Acetabular dysplasia: the acetabular angle. *J Bone Joint Surg Br* 1961;43-B(2):268–272
- 72 Jamali AA, Mladenov K, Meyer DC, et al. Anteroposterior pelvic radiographs to assess acetabular retroversion: high validity of the “cross-over-sign”. *J Orthop Res* 2007;25(6):758–765
- 73 Reynolds D, Lucas J, Klaue K. Retroversion of the acetabulum. A cause of hip pain. *J Bone Joint Surg Br* 1999;81(2):281–288
- 74 Tönnis D, Heinecke A. Acetabular and femoral anteversion: relationship with osteoarthritis of the hip. *J Bone Joint Surg Am* 1999;81(12):1747–1770
- 75 Reikerås O, Bjerkreim I, Kolbenstvedt A. Anteversion of the acetabulum and femoral neck in normals and in patients with osteoarthritis of the hip. *Acta Orthop Scand* 1983;54(1):18–23
- 76 McKibbin B. Anatomical factors in the stability of the hip joint in the newborn. *J Bone Joint Surg Br* 1970;52(1):148–159
- 77 Li PL, Ganz R. Morphologic features of congenital acetabular dysplasia: one in six is retroverted. *Clin Orthop Relat Res* 2003;416:245–253
- 78 Salter RB. The classic. Innominate osteotomy in the treatment of congenital dislocation and subluxation of the hip by Robert B. Salter. *J Bone Joint Surg. (Brit)* 43B:3:518, 1961. *Clin Orthop Relat Res* 1978;137(137):2–14
- 79 Kalberer F, Sierra RJ, Madan SS, Ganz R, Leunig M. Ischial spine projection into the pelvis: a new sign for acetabular retroversion. *Clin Orthop Relat Res* 2008;466(3):677–683
- 80 Nötzli HP, Wyss TF, Stoecklin CH, Schmid MR, Treiber K, Hodler J. The contour of the femoral head-neck junction as a predictor for the risk of anterior impingement. *J Bone Joint Surg Br* 2002;84(4):556–560
- 81 Meyer DC, Beck M, Ellis T, Ganz R, Leunig M. Comparison of six radiographic projections to assess femoral head/neck asphericity. *Clin Orthop Relat Res* 2006;445:181–185
- 82 Nepple JJ, Martel JM, Kim YJ, Zaltz I, Clohisy JC; ANCHOR Study Group. Do plain radiographs correlate with CT for imaging of cam-type femoroacetabular impingement? *Clin Orthop Relat Res* 2012;470(12):3313–3320
- 83 Pollard TC, Villar RN, Norton MR, et al. Femoroacetabular impingement and classification of the cam deformity: the reference interval in normal hips. *Acta Orthop* 2010;81(1):134–141
- 84 Ito K, Minka MA II, Leunig M, Werlen S, Ganz R. Femoroacetabular impingement and the cam-effect. A MRI-based quantitative anatomical study of the femoral head-neck offset. *J Bone Joint Surg Br* 2001;83(2):171–176
- 85 Gelberman RH, Cohen MS, Shaw BA, Kasser JR, Griffin PP, Wilkinson RH. The association of femoral retroversion with slipped capital femoral epiphysis. *J Bone Joint Surg Am* 1986;68(7):1000–1007
- 86 Tönnis D, Heinecke A. Diminished femoral antetorsion syndrome: a cause of pain and osteoarthritis. *J Pediatr Orthop* 1991;11(4):419–431

- 87 Saikia KC, Bhuyan SK, Rongphar R. Anthropometric study of the hip joint in northeastern region population with computed tomography scan. *Indian J Orthop* 2008;42(3):260–266
- 88 Mesgarzadeh M, Revesz G, Bonakdarpour A. Femoral neck torsion angle measurement by computed tomography. *J Comput Assist Tomogr* 1987;11(5):799–803
- 89 Sutter R, Dietrich TJ, Zingg PO, Pfirrmann CW. Femoral ante-torsion: comparing asymptomatic volunteers and patients with femoroacetabular impingement. *Radiology* 2012;263(2):475–483
- 90 Maheshwari AV, Zlowodzki MP, Siram G, Jain AK. Femoral neck anteversion, acetabular anteversion and combined anteversion in the normal Indian adult population: a computed tomographic study. *Indian J Orthop* 2010;44(3):277–282
- 91 Kim HD, Lee DS, Eom MJ, Hwang JS, Han NM, Jo GY. Relationship between physical examinations and two-dimensional computed tomographic findings in children with intoeing gait. *Ann Rehabil Med* 2011;35(4):491–498
- 92 Schneider B, Laubenberger J, Jemlich S, Groene K, Weber HM, Langer M. Measurement of femoral antetorsion and tibial torsion by magnetic resonance imaging. *Br J Radiol* 1997;70(834):575–579
- 93 Tomczak RJ, Guenther KP, Rieber A, Mergo P, Ros PR, Brambs HJ. MR imaging measurement of the femoral antetorsional angle as a new technique: comparison with CT in children and adults. *AJR Am J Roentgenol* 1997;168(3):791–794
- 94 Coleman SS. Diagnosis of congenital dysplasia of the hip in the newborn infant. *J Am Med Assoc* 1956;162(6):548–554
- 95 Eckhoff DG. Variation in femoral anteversion. *Clin Anat* 1994;7(2):72–75
- 96 Wiberg G. Studies on dysplastic acetabula and congenital subluxation of the hip joint. With special reference to the complication of osteoarthritis. *Acta Chir Scand* 1939;83(Suppl 58):28–38
- 97 Maruyama M, Feinberg JR, Capello WN, D'Antonio JA. The Frank Stinchfield Award: Morphologic features of the acetabulum and femur: anteversion angle and implant positioning. *Clin Orthop Relat Res* 2001;(393):52–65
- 98 Toogood PA, Skalak A, Cooperman DR. Proximal femoral anatomy in the normal human population. *Clin Orthop Relat Res* 2009;467(4):876–885
- 99 Buller LT, Rosneck J, Monaco FM, Butler R, Smith T, Barsoum WK. Relationship between proximal femoral and acetabular alignment in normal hip joints using 3-dimensional computed tomography. *Am J Sports Med* 2012;40(2):367–375
- 100 Hetsroni I, Dela Torre K, Duke G, Lyman S, Kelly BT. Sex differences of hip morphology in young adults with hip pain and labral tears. *Arthroscopy* 2013;29(1):54–63